Electronic Supplementary Material (ESI) for Journal of Materials Chemistry C.

Supporting Information

Stable self-powered ultraviolet photodetector using $CH_3NH_3PbCl_3$ with weak-light detection capacity under working condition

Zhirong Liu,[†] *Zhiyong Liu,*[†] *Qiang Sun,*[†] *Tao Zhang,*[†] *Haixuan Yu,*[†] *Xuning, Zhang,*[†] *Letian Dai,*[†] *Guanglan Liao,*[†] *Yan Shen,*[†] *Xiao-Li Zhang,*[‡] *Jun Zhu,*[§] *Mingkui Wang*[*, †]

[†] Wuhan National Laboratory for Optoelectronics, Huazhong University of Science and Technology, 1037 Luoyu Road, Wuhan 430074, Hubei, P. R. China

[‡] State Centre for International Cooperation on Designer Low-Carbon & Environmental Materials, School of Materials Science and Engineering, Zhengzhou University, 450001, P. R. China.

[§] Special Display and Imaging Technology Innovation Center of Anhui Province, State Key Lab of Advanced Display Technology, Key Lab of Advance Functional Materials and Devices of Anhui Province, Academy of Opto-Electric Technology, Hefei University of Technology, 193 Tunxi Road, Hefei, 230009, P. R. China.

Materials: $PbCl_2$ (99.999%) and ethylene glycol (EG) was purchased from Alladdin reagent. PEDOT:PSS was purchased from Xi'an p-OLED. Unless specified, all the reagents and materials were purchased from Sigma-Aldrich. All the reagents were used directly without any further purification.

Preparation of CH_3NH_3Cl powder: 20 mL ethanol and 16.15 mL hydrochloric acid were mixed in flask (100 mL) and stirred for 10 min in ice bath. Then the methylamine solution of 15 mL were dropped slowly by constant pressure funnel, stirring for 2 h at 0 ℃. After hydrochloric acid and methylamine were fully reacted, the solvent was evaporated through rotary evaporator, converting to white powder. The powder was washed by ether 3 times, and then dissolved in ethanol for recrystallization to get white crystals.

Fabrication of $CH_3NH_3PbCl_3$ film and device: EG was added into solvent as solvent additive to selectively dissolve CH_3NH_3Cl instead of $PbCl_2$. Ethyl acetate was introduced as anti-solvents to increase the nucleation sites and form a dense film[1]. Here, 54 mg CH_3NH_3Cl and 222.5 mg $PbCl_2$ were dissolved in 1 mL DMF-DMSO (1:1 in volume) with 0.2% EG to get 0.8 M $CH_3NH_3PbCl_3$ precursor solution. The mixture was stirred in glove box overnight to get transparent solution. Before use, the solution was filtered using a 0.22 µm filter. A PEDOT:PSS hole transport layer (HTL) was prepared by spin-coating of PEDOT:PSS solution at 4000 rpm for 40 s under the annealing conditions of 140 ℃ for 40 min in an ambient atmospheric environment. The samples were transferred to glove box for perovskite deposition after cooling to room temperature. The precursor solution was spin-coated by 5000 rpm for 20 s, and ethyl acetate was casted as anti-solution before the end of 10 s. The deposited perovskite films were annealed for 30 min. $PC_{61}BM$ (20 mg mL^{-1}) in chlorobenzene was spin-coated onto the perovskite films at 2000 rpm for 40 s as electron transport layer (ETL). BCP was used as hole blocking layer by spin-coating at 4000 rpm for 40 s. At last, a 100-nm silver counter electrode was thermally deposited onto the BCP layer under vacuum below 8×10^{-4} Pa.

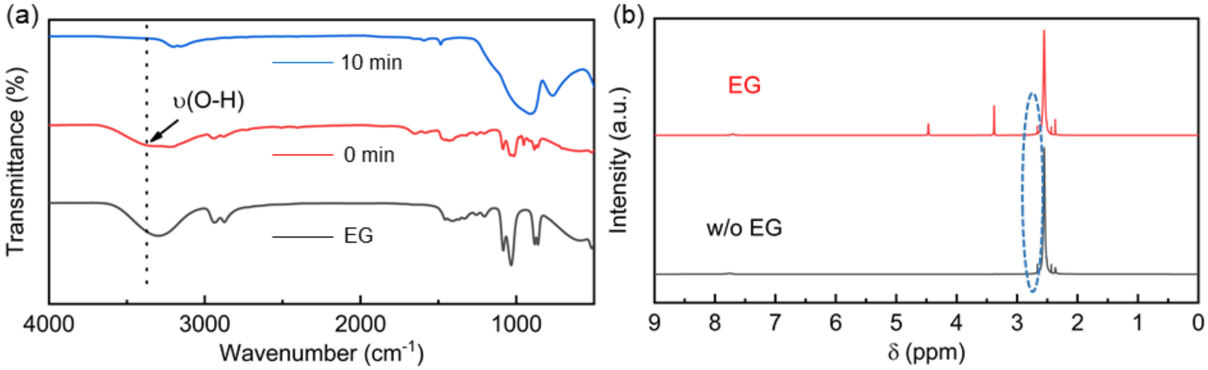

Figure S1 (a) FTIR transmittance spectra for the EG treated $CH_3NH_3PbCl_3$ following by annealing for 10 min, without annealing, and pure EG. (b) ^1H NMR spectra of perovskite precursor components with and without EG in deuterium with DMSO

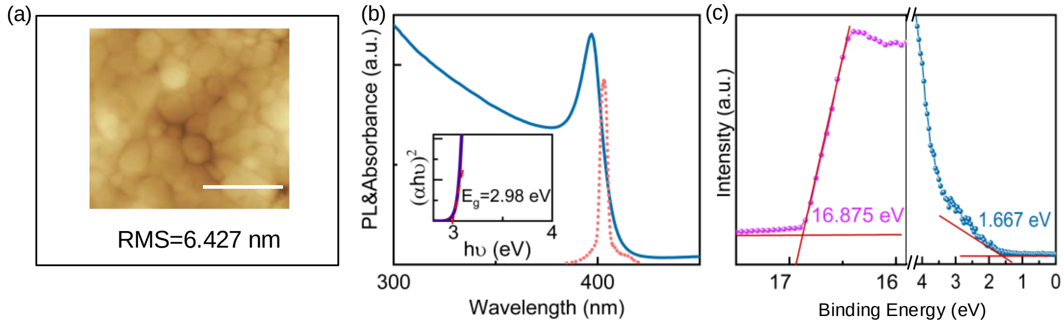

Figure S2. (a) AFM image $CH_3NH_3PbCl_3$ film, the scale bar is 1 μm; (b) V-vis absorption (solid line) and photoluminescence spectra (dotted line) of the CH3NH3PbCl3 film (the inset: the bandgap derived from the absorbance measurement); (c) UPS characteristic of the $CH_3NH_3PbCl_3$ film on Glass/ITO/PEDOT:PSS substrate.

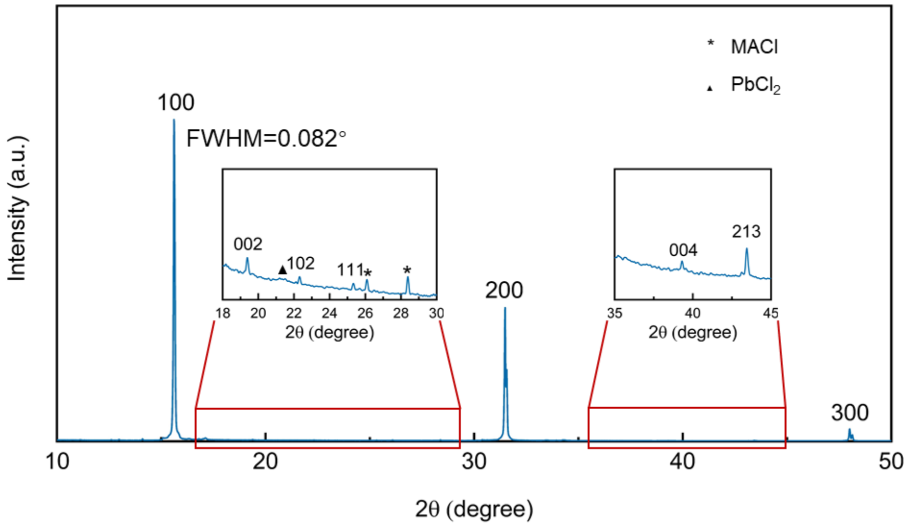

Figure S3 XRD patterns of $CH_3NH_3PbCl_3$ film fabricated with 0.2% EG.

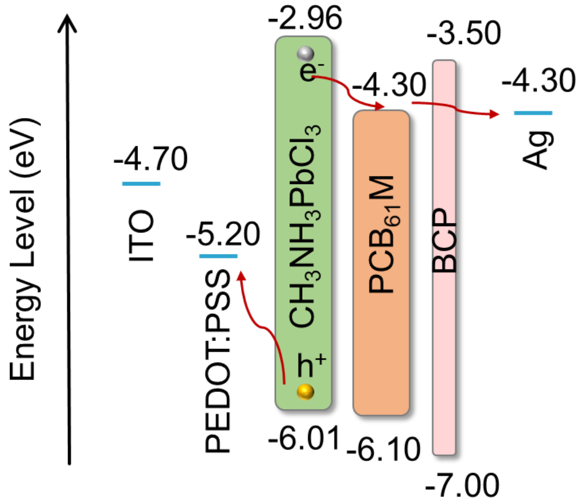

Figure S4. Energy level diagram of individual layers used in $CH_3NH_3PbCl_3$ UV detector.

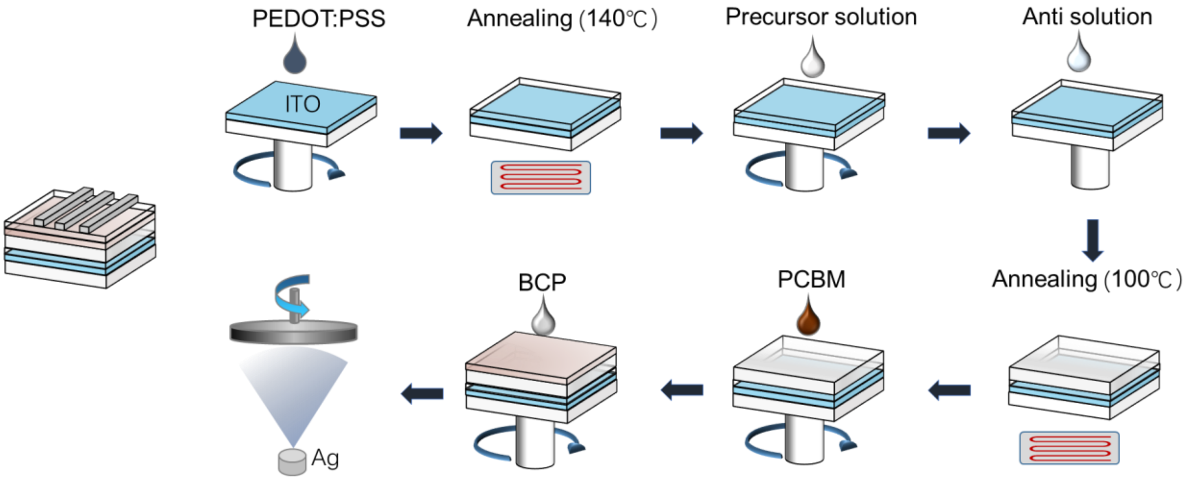

Figure S5 Schematic diagram of fabrication process of $CH_3NH_3PbCl_3$ UV photodetector.

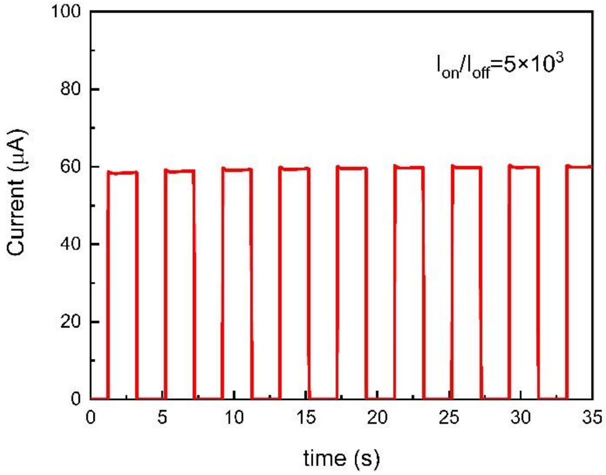

Figure S6. Temporal response of the device toward square wave signals under illumination by 375 nm laser with intensity of 24.6 mW cm^{-2}.

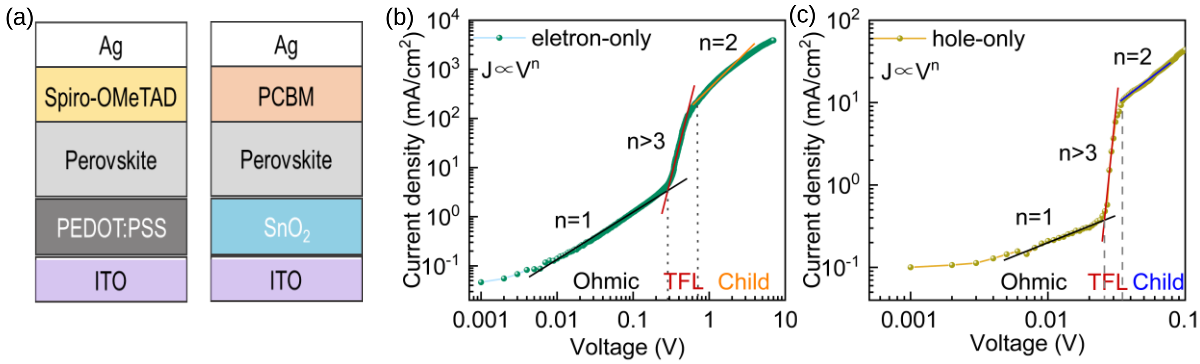

Figure S7. Space charge limit current characteristic of $CH_3NH_3PbCl_3$ films; (a) diagram of device structure of hole-only (left) and electron-only device (right); (b) *I-V* curve of electron-only device; (c) *I-V* curve of hole-only device.

Space charge limit current model (SCLC) measurement: The electron-only devices and hole-only devices (figure S4a) were measured individually. The *J-V* curve was separated into various parts by different n ($J \propto V^n$). When the bias was below V_{TFL}, the *J-V* curve follows Ohm's law, where $J \propto V^{n=1}$. When the bias increases, the *J-V* characteristic changes, where the current density rises sharply ($J \propto V^{n>3}$). At this stage, the trap states are occupied by the charge carriers, which is so called trap-filled limit (TFL). The trap density (n_{traps}) can be gotten through the relationship between V_{TFL} and n_{traps},

$$n_{traps} = \frac{2\varepsilon\varepsilon_0 V_{TFL}}{ed^2} \quad \text{(S1)}$$

where ε_0 is the vacuum permittivity and ε is the dielectric constant of $CH_3NH_3PbCl_3$ given by 23.9[2], *d* is the thickness of perovskite film and e is the elementary charge respectively. V_{TFL} is the voltage required to support the total trapped space-charge, 0.220 V for electron-only device and 0.025 V for hole-only device. By means of Equation.S1, we can estimate electron trap density (n_e) and hole trap density (n_h) to be 7.92×10^{15} cm^{-3} and 9.07×10^{14} cm^{-3}. When bias rises higher, the space-charge effect occurs, where the current is limited by space-charge ($J \propto V^{n=2}$), fitting Mott−Gurney law,

$$J = \frac{9}{8}\varepsilon\varepsilon_0\mu\frac{V^2}{d^3} \quad \text{(S2)}$$

where *J* is the current density and *V* is the voltage applied. The carrier mobility (μ) was extracted to be 9.26×10^{-3} $cm^2V^{-1}s^{-1}$ (μ_e) and 4.52×10^{-4} $cm^2V^{-1}s^{-1}$ (μ_h).

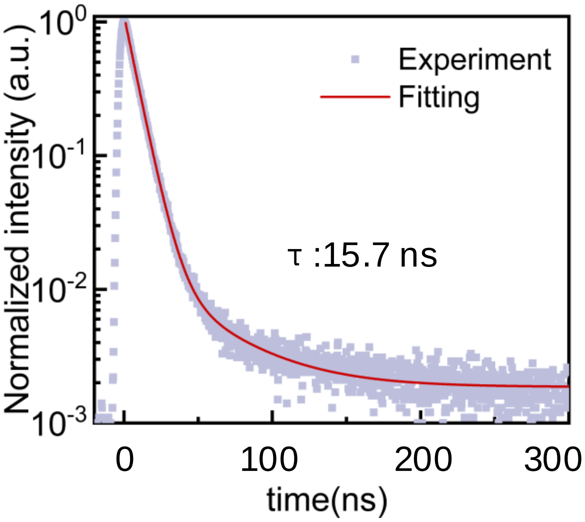

Figure S8. Time-resolved photoluminescence spectrum of the $CH_3NH_3PbCl_3$ film.

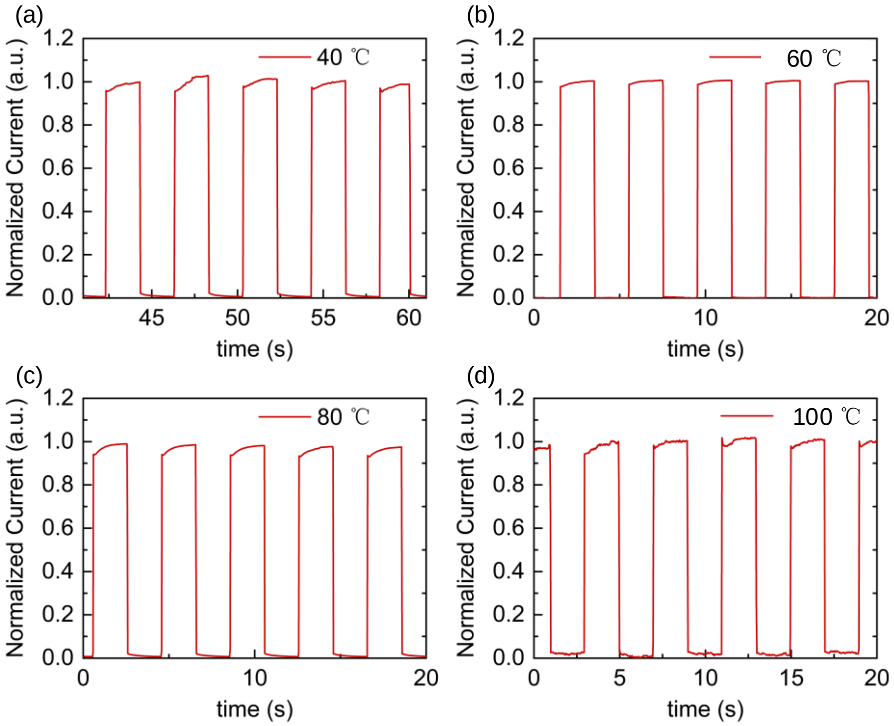

Figure S9. Response curves of the device by heating at different temperature (the response photo current was normalized by current measured at 25 ℃).

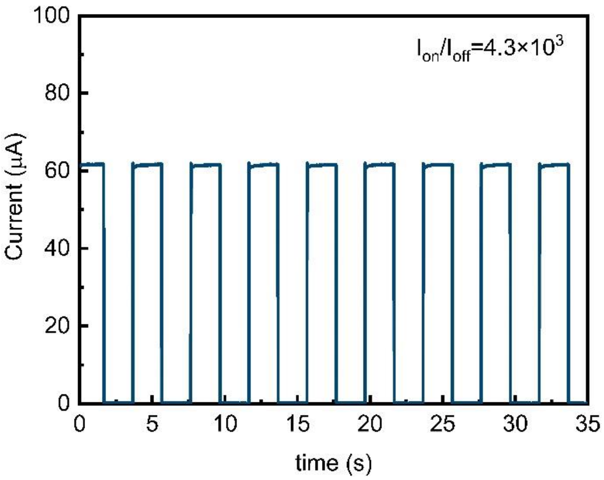

Figure S10. Response curves of the flexible device constructed on Polyethylene naphthalate substrate under illumination by laser diode at 375 nm with an intensity of 24.6 mW cm^{-2}.

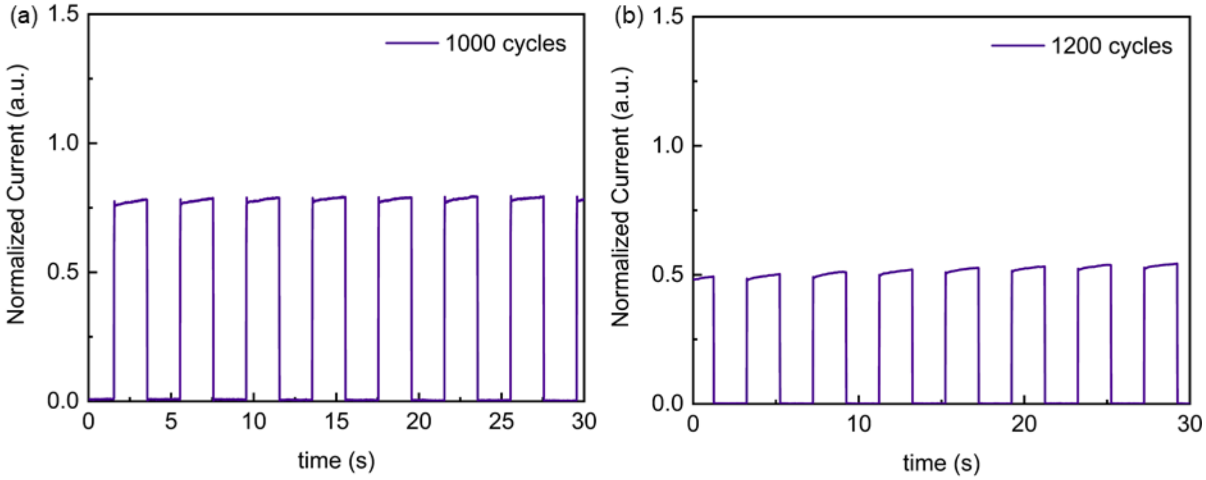

Figure S11. Response curves of the flexible device after 1000 (a) and 1200 (b) bending cycles.

References

1 J. Chen, J. Song, F. Huang, H. Li, S.Liu, M. Wang, and Y. Shen. *J. Phys. Chem. C* **2017,** 121, 17053–17061.

2 A. Poglitsch, D. Weber. *J. Chem. Phys.* **1987**, 87, 6373-6378.